JACS
JOURNAL OF THE AMERICAN CHEMICAL SOCIETY
Article
pubs.acs.org/JACS

From C_{60} to Infinity: Large-Scale Quantum Chemistry Calculations of the Heats of Formation of Higher Fullerenes

Bun Chan,*[,†,‡] Yukio Kawashima,[‡] Michio Katouda,[‡] Takahito Nakajima,[‡] and Kimihiko Hirao[‡]

[†]School of Chemistry, University of Sydney, Sydney, New South Wales 2006, Australia
[‡]RIKEN Advanced Institute for Computational Science, 7-1-26 Minatojima-minami-machi, Chuo-ku, Kobe, Hyogo 650-0047, Japan

Supporting Information

ABSTRACT: We have carried out large-scale computational quantum chemistry calculations on the K computer to obtain heats of formation for C_{60} and some higher fullerenes with the DSD-PBE-PBE/cc-pVQZ double-hybrid density functional theory method. Our best estimated values are 2520.0 ± 20.7 (C_{60}), 2683.4 ± 17.7 (C_{70}), 2862.0 ± 18.5 (C_{76}), 2878.8 ± 13.3 (C_{78}), 2946.4 ± 14.5 (C_{84}), 3067.3 ± 15.4 (C_{90}), 3156.6 ± 16.2 (C_{96}), 3967.7 ± 33.4 (C_{180}), 4364 (C_{240}) and 5415 (C_{320}) kJ mol^{-1}. In our assessment, we also find that the B3-PW91-D3BJ and BMK-D3(BJ) functionals perform reasonably well. Using the convergence behavior for the calculated per-atom heats of formation, we obtained the formula $\Delta_f H$ per carbon = $722n^{-0.72}$ + 5.2 kJ mol^{-1} (n = the number of carbon atoms), which enables an estimation of $\Delta_f H$ for higher fullerenes more generally. A slow convergence to the graphene limit is observed, which we attribute to the relatively small proportion of fullerene carbons that are in "low-strain" regions. We further propose that it would take tens, if not hundreds, of thousands of carbons for a fullerene to roughly approach the limit. Such a distinction may be a contributing factor to the discrete properties between the two types of nanomaterials. During the course of our study, we also observe a fairly reliable means for the theoretical calculation of heats of formation for medium-sized fullerenes. This involves the use of isodesmic-type reactions with fullerenes of similar sizes to provide a good balance of the chemistry and to minimize the use of accompanying species.

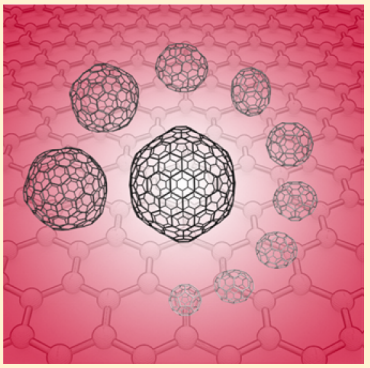

INTRODUCTION

There is a vast and rapidly growing interest in carbon-based nanomaterials, and C_{60} is still at the center of this technological revolution.[1] It is therefore of great significance to have accurate knowledge of its property.[2,3] Despite its importance, one of the most fundamental properties of C_{60}, namely its heat of formation ($\Delta_f H$), is still not determined experimentally with a good precision (with an uncertainty of 100 kJ mol^{-1}).[4]

Recently, the $\Delta_f H$ value for C_{60} has been re-evaluated[5,6] using state-of-the-art computational chemistry methods as applied to isodesmic-type reactions.[7,8] Specifically, in ref 5, contemporary double-hybrid density functional theory (DH-DFT) method was employed, and in ref 6 a refined value was obtained using even higher-level composite protocol. Despite the improved accuracy of the calculated value versus the experimental one, it was initially suggested that it might still be associated with a seemingly sizable uncertainty.[5] We note that a value for the uncertainty was not stated in ref 5, but the data was later interpreted and an uncertainty of 13.6 kJ mol^{-1} was suggested accordingly.[9] The recent study by Wan and Karton,[6] while conducted at a very impressive level of theory, does not include a quoted uncertainty. It is thus of interest to examine in more detail this quantity. In addition, given that the use of high-level methodologies, e.g., CCSD(T) employed in ref 6, while achievable, remains computationally demanding for C_{60} and is perhaps prohibitive for larger fullerenes, to further accurate quantum chemistry study of fullerenes, it is important to ask: how sensitive is the calculated $\Delta_f H$ with respect to methods that are computationally accessible?

The present study aims to address these points by critically compare a series of methods related to the DH-DFT procedure used in ref 5, as well as to assess computationally less-demanding procedures. Furthermore, we will employ our chosen methods to calculate the heats of formation for higher fullerenes, for which neither accepted experimental nor accurate theoretical values yet exist. We hope that the results of this investigation will, not only provide the best theoretical estimate to date for these quantities, but also yield fundamental insights into the chemistry of these species. Thus, we aim to complement other studies, e.g., by Cioslowski and co-workers[10] and by Schwerdtfeger and co-workers[11] regarding the theoretical calculation, topology, and convergence behavior, of some (higher) fullerenes (up to C_{980} in ref 11).

COMPUTATIONAL DETAILS

Standard density functional theory (DFT) and double-hybrid DFT (DH-DFT) calculations were carried out with Gaussian 09,[12] NTChem 2013,[13] and Orca 3.1.[14] Geometries, zero-point vibrational energies (ZPVE), thermal corrections for 298 K enthalpies (ΔH_{298-0}), and benchmark total energies were taken from ref 5 where available. For the additional systems, geometries, and vibrational frequencies

Received: December 6, 2015
Published: January 22, 2016

DOI: 10.1021/jacs.5b12518
J. Am. Chem. Soc. 2016, 138, 1420−1429

were mainly obtained at the B3-LYP/6-31G(2df,p) level. The initial structures for geometry optimizations were taken from the Supporting Information of ref 15. For higher fullerenes for which multiple isomers exist, we have examined the forms that were found to be of the lowest energies.[10,16−19] They correspond to isomers 3 (C_{78}), 22 (C_{84}), 45 (C_{90}) and 183 (C_{96}) according to the numbering scheme of ref 2, and have symmetries of C_{2v} for C_{78}, D_2 for C_{84}, C_2 for C_{90} and D_2 for C_{96}. Literature scale factors[20] were applied to the frequencies in the calculation of ZPVE and ΔH_{298-0} values. During the course of our investigation, we have briefly examined the use of alternative procedures for geometry optimizations and the associated frequency calculations. We find that the use of B3-LYP/6-31G(d) quantities led to very small differences from the B3-LYP/6-31G(2df,p) values. In addition, the use of B-LYP/6-31G(d) and even the semiempirical PDDG method,[21] once the scale factors were redetermined for the particular case of medium-sized fullerenes, gave ZPVE and ΔH_{298-0} values that agree well with the B3-LYP/6-31G(2df,p) quantities. For some of the largest systems, PDDG frequencies were employed for the calculation of ZPVE and ΔH_{298-0} using scale factors of 0.8749 (ZPVE) and 0.9288 (ΔH_{298-0}).

The previous high-level computational study, specifically ref 5, employed a series of isodesmic-type reactions for the calculation of the $\Delta_f H$ of C_{60} using the straightforward thermochemical cycle: reaction energy = $\Sigma\ \Delta_f H$(products) − $\Sigma\ \Delta_f H$(reactants) together with computed reaction energies and known experimental or high-level theoretical $\Delta_f H$ values for the accompanying species in the equations. The same approach will be used in the present study. The highest-level computational procedure used in that study for C_{60} was the DH-DFT method DSD-PBE-P86[22] (DSD signifies the incoporation of Dispersion correction and Spin-component scaling into a Double-hybrid DFT) in conjunction with the quadruple-ζ cc-pVQZ basis set. In the present study, a more diverse range of related DH-DFT procedures will be examined. These include B2-PLYP,[23] B2GP-PLYP,[24] B2K-PLYP,[25] PWP-B95,[26] DuT-D3,[27] DSD-PBE-P86,[22] DSD-B-P86[22] and DSD-PBE-PBE.[22] We will assess their performance in combination with cc-pVQZ as well as the smaller cc-pVTZ basis set. We note that the definition of DSD-PBE-P86, DSD-B-P86 and DSD-PBE-PBE has been slightly revised[28] since the publication of ref 5. In the present study, we use the revised parameters reported in ref 28.

The computationally less demanding methods that will be assessed include a range of popular and contemporary DFT procedures, such as B3-LYP,[29] B3-PW91,[30] CAM-B3-LYP,[31] PBE1-PBE,[32] TPSSh,[33] LC-ωPBE,[34] B98,[35] BMK,[36] ωB97X,[37] PW6-B95,[38] M06-2X[39] and MN12-SX.[40] Such a diverse set of DFT methods will complement a recent study,[9] which assessed a limited number of procedures on the same set of reactions related to the $\Delta_f H$ of C_{60}. For both DFT and DH-DFT procedures, the effect of the inclusion of dispersion corrections will be examined. To this end, unless otherwise noted, we use the D3(BJ)[41] methodology in the present study. For some functionals, the D3[42] and D2[43] dispersion corrections were employed. For the sake of simplicity, we will refer to dispersion-corrected DFT procedures simply as DFT-D.

RESULTS AND DISCUSSION

General Discussion. A set of isodesmic-type reactions were used in ref 5. To obtain $\Delta_f H$ values for small polycyclic aromatic hydrocarbons (PAHs) that are necessary for the calculation of $\Delta_f H$ of C_{60}, reactions of the general formula

$$\text{PAH} + m\ C_2H_4 \rightarrow n\ \text{benzene}$$

were recommended among a larger set of reactions. Such a choice was based on considerations of a balance between minimizing the uncertainties of the experimental quantities employed and conserving molecular fragments between reactants and products. Specifically, the four recommended reactions are

$$\text{naphthalene}(C_{10}H_8) + C_2H_4 \rightarrow 2\ \text{benzene} \quad (1)$$

$$\text{phenanthrene}(C_{14}H_{10}) + 2C_2H_4 \rightarrow 3\ \text{benzene} \quad (2)$$

$$\text{triphenylene}(C_{18}H_{12}) + 3C_2H_4 \rightarrow 4\ \text{benzene} \quad (3)$$

$$\text{corannulene}(C_{20}H_{10}) + 5C_2H_4 \rightarrow 5\ \text{benzene} \quad (4)$$

These reactions correspond roughly to level two of the "connectivity-based hierarchy" scheme, i.e., CBH-2, of Ramabhadran and Raghavachari.[8] The $\Delta_f H$ values for C_{60} were obtained using a similar set of isodesmic-type reactions:

$$C_{60} + 10\ \text{benzene} \rightarrow 6\ \text{corannulene} \quad (5)$$

$$C_{60} + 10\ \text{naphthalene} \rightarrow 8\ \text{corannulene} \quad (6)$$

$$C_{60} + 10\ \text{phenanthrene} \rightarrow 10\ \text{corannulene} \quad (7)$$

$$C_{60} + 10\ \text{triphenylene} \rightarrow 12\ \text{corannulene} \quad (8)$$

Notably, all of the reactions 5−8 involve corannulene, which was used to preserve the character of the curvature in C_{60}. As C_{60} consists of connected five- and six-membered rings, it is appropriate to consider these cyclic structures as the fundamental components in isodesmic-type reactions. In this sense, reactions 5−8 could be loosely classified as CBH-1 for reaction 5 and, to different degrees, higher-order CBH for reactions 6−8. Likewise, under the alternative schemes of Wheeler, Houk, Schleyer and Allen,[7] these reactions would rank approximately at levels 1−4. On the other hand, if one employs conventional definitions of isodesmic-type reactions of refs 7 and 8, i.e., using C−C and C=C bonds as basic building blocks, then all of the reactions 5−8 would be catergorized as fairly high order under their hierarchy schemes.

In the present study, the reactions 1−8 are examined with a larger range of DFT and DH-DFT procedures. We use reactions 1−4, for which high-level W1h-type[44−46] benchmark values are available,[5] to assess the performance of lower-cost procedures. We then investigate reactions 5−8 in order to gain a better appreciation of the uncertainty involved in the calculation of $\Delta_f H$ for C_{60} using these DFT and DH-DFT procedures.

Performance of DFT and DH-DFT Procedures for Reactions 1−4. We now assess how the various methods fare for the calculation of reaction energies against the W1h benchmark values provided in ref 5. Table 1 shows the mean absolute deviations (MADs) correspond to DFT and DH-DFT computations carried out in conjunction with the cc-pVTZ and cc-pVQZ basis sets, and with and without dispersion corrections. It is apparent that, as one might suspect, there is only small differences between the results obtained with the triple- and quadruple-ζ basis sets for the various DFT methods, but the distinctions are somewhat more significant for the DH-DFT procedures. Interestingly, the use of the larger basis set often do not lead to smaller MADs than those obtained with the smaller basis set. This is the case for both DFT and DH-DFT methods, and both with and without dispersion corrections, for this set of reaction energies.

In comparison with the relative mild basis set effect, the inclusion of dispersion correction has a notable effect on the MADs. In this case, the use of such an additional component always leads to a better overall agreement with the benchmark values for this test set, with the effect more prominent for the DFT than for the DH-DFT procedures. The more significant improvement for DFT than for DH-DFT methods is consistent with the parametrization of the dispersion corrections, which

DOI: 10.1021/jacs.5b12518
J. Am. Chem. Soc. 2016, 138, 1420−1429

Table 1. Mean Absolute Deviations (kJ mol^{-1}) from Benchmark W1h Reaction Energies for Reactions 1−4 for the Various DFT and DH-DFT Procedures

	no dispersion correction		with dispersion correction[a]	
	cc-pVTZ	cc-pVQZ	cc-pVTZ	cc-pVQZ
DFT methods				
B3-LYP	31.7	32.0	13.4	13.6
B3-PW91	31.9	31.7	11.2	11.0
CAM-B3-LYP	35.1	35.3	21.4	21.6
PBE1-PBE	31.3	31.1	19.1	18.9
TPSSh	28.7	28.5	13.4	13.2
LC-ωPBE	33.8	33.3	19.6	19.0
B98	30.7	30.8	15.2[b]	15.4[b]
BMK	26.7	28.8	9.2	11.3
ωB97X	33.4	33.9	25.6[c]	25.8[c]
PW6-B95	29.5	29.8	20.0	20.3
M06-2X	26.6	26.2	24.8[d]	24.4[d]
MN12-SX	21.9	24.9	–	–
DH-DFT methods				
B2-PLYP	18.3	19.3	8.5	9.5
B2GP-PLYP	16.7	18.0	9.4	10.7
B2K-PLYP	15.7	17.1	–	–
PWP-B95	13.1	16.9	5.6	9.4
DuT-D3	12.3	–	9.4	–
DSD-PBE-P86	8.6	10.0	3.1	4.5
DSD-B-P86	9.5	10.9	2.6	2.7
DSD-PBE-PBE	7.8	9.1	2.4	1.8

[a]D3(BJ) correction unless otherwise noted. [b]The parameters for B97 were used. [c]D2 correction. [d]D3 correction with zero damping.

typically have larger coefficients for both the medium-range and the long-range corrections for the DFT procedures.

The MADs for the DFT-D methods are in a range of approximately 10−25 kJ mol^{-1}. Overall, the smallest MAD achieved by a hybrid DFT is 9.2 kJ mol^{-1} for BMK-D/cc-pVTZ. This is followed by B3-PW91-D for which the MADs are ∼11 kJ mol^{-1}. When DH-DFT methods are included in the tally, the DSD-PBE-PBE/cc-pVQZ procedure shows that best performance for this set with an MAD of 1.8 kJ mol^{-1}. It is noteworthy that all three DSD-type functionals tested in the present study show fairly good performance (∼1.5−5 kJ mol^{-1}), which is notably better than those for the other DH-DFT-D procedures assessed (∼5−10 kJ mol^{-1}). However, for this set of isodesmic reactions, the DSD-PBE-P86/cc-pVQZ (MAD = 4.5 kJ mol^{-1}) protocol that was used in ref 5 is outperformed by both DSD-B-P86 (2.7 kJ mol^{-1}) and DSD-PBE-PBE (1.8 kJ mol^{-1}).

While the MAD values provide an average picture of the performance of the various procedures, it is instructive to examine the deviations for each of the four reactions 1−4. This is shown in Table 2 for the DFT and DH-DFT methods that we consider to be the most accurate. They include hybrid functionals B3-PW91-D and BMK-D, and DH-DFT procedures DSD-PBE-P86, DSD-B-P86 and DSD-PBE-PBE. It is apparent that, in all of these cases, the major source of deviation comes from reaction 4, i.e., corannulene + 5 C_2H_4 → 5 benzene. Among the four reactions, this is the only one that involves corannulene, while reactions 1−3 consist exclusively of planar substrates. Presumably, the curvature of corannulene leads to a less good error compensation for reaction 4, which is reflected in the notably larger deviations.

Table 2. Deviations (kJ mol^{-1}) from Benchmark W1h Reaction Energies for Reactions 1−4 for B3-PW91-D, BMK-D, DSD-PBE-P86, DSD-B-P86 and DSD-PBE-PBE

	B3-PW91-D	BMK-D	DSD-PBE-P86	DSD-B-P86	DSD-PBE-PBE
			cc-pVTZ		
1	−1.8	−2.0	0.1	0.4	1.2
2	−4.9	−2.6	−0.1	0.8	2.0
3	−9.0	−4.0	−0.5	1.5	2.6
4	−29.0	−28.0	−11.7	−7.8	−3.6
			cc-pVQZ		
1	−1.9	−3.2	−0.6	−0.2	0.6
2	−4.9	−4.9	−1.4	−0.5	0.9
3	−8.9	−7.2	−2.6	−0.5	0.7
4	−28.5	−30.0	−13.4	−9.5	−5.1

The performances of the three DH-DFT procedures are quite similar for reactions 1−3, with deviations (in many cases, substantially) less than 3 kJ mol^{-1}. However, for reaction 4, the differences between them are more apparent, with DSD-PBE-PBE yielding the smallest deviations. Again, it is noteworthy that, perhaps due to cancellation of error, the deviations for the larger cc-pVQZ basis set are not always smaller than those for cc-pVTZ. Overall, BMK-D/cc-pVTZ appears to be the best hybrid-meta DFT method in Table 2, and we deem DSD-PBE-PBE to be the best DH-DFT in these cases. Although the choice of basis set is less clear-cut for DSD-PBE-PBE, we prefer cc-pVQZ due to the smaller deviations associated with reactions 1−3, as well as it being closer to the complete-basis-set limit.

Sensitivity of the Calculated Reaction Energies to the Functional. We now examine more generally the sensitivity of the reaction energies for reactions 1−8 to the choice of DFT and DH-DFT procedures. We wish that this would provide a picture of the smallest uncertainty that may be achieved with the current generation of DFT and DH-DFT methods for these reactions. In Table 3 the results for the B3-PW91-D and BMK-D hybrid DFT methods are included, as well as those for the DH-DFT procedures DSD-PBE-P86, DSD-B-P86 and DSD-PBE-PBE. Because the basis set effects are not excessive for these procedures, for the sake of simplicity, we show only the results obtained with cc-pVQZ.

Table 3. Calculated Vibrationless Reaction Energies (kJ mol^{-1}) for Reactions 1−8 Obtained with Selected DFT and DH-DFT Procedures in Conjunction with the cc-pVQZ Basis Set, and Standard Deviation (SD) for Each Reaction

	B3-PW91-D	BMK-D	DSD-PBE-P86	DSD-B-P86	DSD-PBE-PBE	SD
1	−41.2	−42.5	−39.9	−39.5	−38.7	1.5
2	−73.5	−73.5	−70.0	−69.1	−67.7	2.6
3	−111.0	−109.3	−104.7	−102.6	−101.4	4.2
4	−383.7	−385.2	−368.6	−364.7	−360.3	11.3
5	−507.1	−486.1	−487.0	−470.3	−474.7	14.3
6	−151.6	−140.2	−148.5	−136.3	−141.0	6.3
7	293.1	320.1	287.0	297.9	289.2	13.3
8	685.1	731.8	677.9	692.0	673.4	23.4

We first note that for reactions 1−3, the narrow spread of calculated reaction energies with the different methods (and the associated deviations in Table 2) is reflected in their small standard deviation (SD) values, with the largest one being 4.2

DOI: 10.1021/jacs.5b12518
J. Am. Chem. Soc. 2016, 138, 1420−1429

kJ mol^{-1} for reaction 3. The relatively more challenging case of reaction 4 has a notably larger SD of 11.3 kJ mol^{-1}. It is noteworthy that SD values in Table 3 appear to have reasonable correlations with the magnitudes of the deviations shown in Table 2. Such a connection is shown in Figure 1, with R^2 values

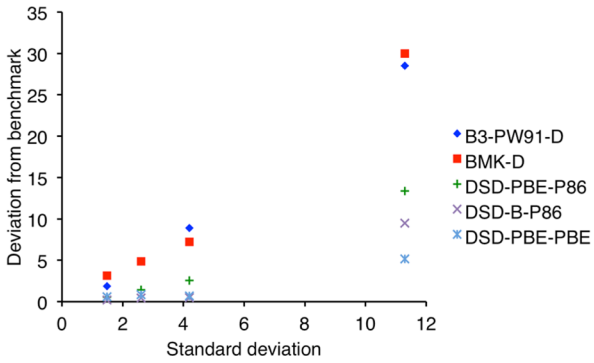

Figure 1. Absolute deviations (kJ mol^{-1}) from benchmark values for the calculated reaction energies with the cc-pVQZ basis set for reactions 1−4, versus the associate standard deviations (kJ mol^{-1}) over the five theoretical methods.

of 1.00 (B3-PW91-D), 0.99 (BMK-D), 0.99 (DSD-PBE-P86), 0.95 (DSD-B-P86) and 0.94 (DSD-PBE-PBE). While the observation of larger SDs for the more difficult cases (i.e., larger deviations) is not entirely unexpected, the semiquantitative trends have enabled us to "roughly guess" the uncertainties for the various theoretical methods for reactions where higher-level benchmark values are not available.

We now turn our attention to reactions 5−8. It is apparent that reaction 6, with its smallest SD value of 6.3 kJ mol^{-1}, is likely to provide the most accurate reaction energies as calculated by the various DFT and DH-DFT methods. At the other end of the spectrum, reaction 8 has the largest SD of 23.4 kJ mol^{-1}. Judging from Figure 1, if one uses the seemingly most accurate DSD-PBE-PBE method, the uncertainty associated with the calculation of reaction 6 is, conservatively, likely to be below 5 kJ mol^{-1}. For reactions 5 and 7, the uncertainly can be expected to be larger, and we anticipate the value to be around 7 kJ mol^{-1}. The use of DSD-PBE-P86 and DSD-B-P86 that perform less well for reactions 1−4 may be associated with larger uncertainties of over 10 kJ mol^{-1} for reactions 5, 7 and (especially) 8, but their calculations of reaction 6 may remain relatively accurate.

We emphasize that the spread of reaction energies obtained with the various methods is by-no-means an infallible approach for obtaining a rough estimation of the uncertainty, and the general reliablility of such a methodology may only be established with a more thorough investigation. However, DFT and DH-DFT classes of procedures, in particular with the large wave function contributions in the DSD-type functionals, are likely to have quite different strengths and weaknesses. We therefore believe that our approach would have a reduced chance of false negative when good agreements are observed between all the DFT and DH-DFT procedures. As an aside, we note that our DSD-PBE-P86 values obtained using parameters of ref 28 are not too different from those reported previously[5] using ref 22 parameters.

Heat of Formation of C_{60}. Having assessed the likely uncertainties associated with the use of the various DH-DFT procedures for the calculations of reaction energies for reactions 5−8, we now proceed to provide our best estimate for the heat of formation of C_{60}. To this end, we first note that the quoted uncertainties for the heats of formation for the other species involved in reactions 5−8 increase in the order: benzene (0.3 kJ mol^{-1}) < naphthalene (1.5) < phenanthrene (2.3) < triphenylene (4.4) < corannulene (7.9).[5] Using standard error propagation principles, the uncertainties associated with the Δ_fH values of these species in the calculation of the Δ_fH of C_{60} with reactions 5−8 would be 47.5 (reaction 5), 65.0 (6), 82.3 (7) and 104.5 (8) kJ mol^{-1}! These large uncertainty values are dominated by the fairly significant uncertainty of corannulene. To this end, we note that the corannulene uncertainty of 7.9 kJ mol^{-1} was proposed based on an assumed uncertainty of 7.7 kJ mol^{-1} for the W1h reaction energies, which is based on a 95% confidence interval determined for a set of atomization energies and a compilation of uni- and bimolecular reactions associated with the species involved.

Given the significant contribution of this uncertainty to the total uncertainties for reactions 5−8, we re-examine its value in the present study. We note that for a diverse set of systems,[47] for the W1RO procedure,[48] which is closely related to W1h, the root-mean-square deviations (RMSDs) for bond dissociation energies, heavy atom transfers, isomerizations and nucleophilic substitutions are 3.3, 5.4, 0.8, and 1.3 kJ mol^{-1}, respectively. Thus, reactions that do not involve homolytic bond cleavages have (considerably) smaller uncertainties. We further note that isodesmic-type reactions, such as reactions 1−8 used in the present study, are constructed to conserve the chemistry between reactants and products in order to maximize cancellation of errors. In comparison, the isomerization and nucleophilic substitution reactions in ref 47 do not necessarily have such a desirable feature.

What degree of improvement in accuracy for the calculated reaction energies can we expect from the usage of isodesmic-type reactions? We note that for the reactions examined in ref 7, the MADs for CCSD(T)/cc-pVTZ reaction energies decrease rapidly from ∼150 kJ mol^{-1} for (nonisodesmic) atomization reactions to ∼0.6 kJ mol^{-1} for high-order isodesmic-type reactions. The isodesmic-type reactions in that study typically have multiple reactants and multiple products. Accordingly, the contribution from each species can be expected to be somewhat smaller. We estimate that a pair of reactant plus product is associated with an RMSD of ∼0.4 kJ mol^{-1}. With the even higher-level W1h procedure used previously[5] for obtaining the reaction energies for reactions 1−4, a further improved accuracy seems plausible. Taking these factors into account, we thus deem it reasonably conservative to assume the same RMSD value of 0.4 kJ mol^{-1} for a single pair of reactant plus product within the isodemismic-type reactions 1−4. This corresponds to an associated uncertainty of ∼0.8 kJ mol^{-1}.

For reaction 4 used in the computation of the Δ_fH of corannulene, a total of 11 species are involved. We assume a linear scaling of the uncertainty with the number of these species, and herein proposed a revised uncertainty value of 4.4 kJ mol^{-1}. When this revised uncertainty for the Δ_fH of corannulene is applied to reactions 5−8, the total uncertainties associated with the known Δ_fHs, determined using standard error propagation principles, are 26.6, 38.3, 49.6 and 68.7 kJ mol^{-1}, respectively. Taking the roughly estimated uncertainties for the DSD-PBE-PBE reaction energies of 7, 5, 7 and 10 kJ mol^{-1} into account, we propose Δ_fH values for C_{60} of 2526.8 ±

DOI: 10.1021/jacs.5b12518
J. Am. Chem. Soc. 2016, 138, 1420−1429

27.5, 2502.1 ± 38.6, 2543.5 ± 50.1 and 2471.3 ± 69.5 kJ mol^{-1} for reactions 5−8, respectively (Figure 2).

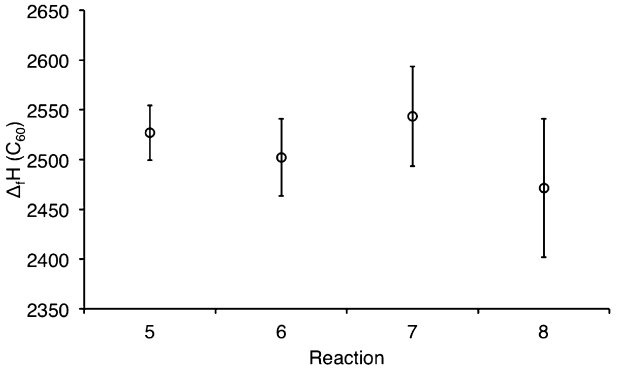

Figure 2. Heat of formation values (kJ mol^{-1}) for C_{60} obtained with DSD-PBE-PBE/cc-pVQZ reaction energies for reactions 5−8.

We now consider the overlapping range of these Δ_fH values, and suggest a final value of 2520.0 ± 20.7 kJ mol^{-1} for the Δ_fH of C_{60}. We note that this is quite close to the values of 2521.6 and 2511.7 kJ mol^{-1} proposed in refs 5 and 6. It is in particularly good agreement with the value of ref 5, which was based on an average of values obtained with reactions 5 and 6 using the original DSD-PBE-P86 procedure.[5] The results obtained in the present study, with a DH-DFT procedure that is slightly more accurate for these systems, and a somewhat more in-depth examination of the uncertainties, further support the previous propositions that the NIST value of 2560 kJ mol^{-1} for Δ_fH (C_{60}) should be revised downward.

Heats of Formation of Medium-Sized Higher Fullerenes. We now proceed to estimate the heats of formation for some higher fullerenes, specifically C_{70}, C_{76}, C_{78}, C_{84}, C_{90} and C_{96}. The former four are of particular practical relevance with their milligram-scale commercial availability (e.g., from Sigma−Aldrich), whereas the latter two are among the largest pristine fullerenes isolated.[49−51]

We again employ isodesmic-type reactions to obtain the Δ_fH values of these species. We use C_{60} and the higher fullerenes themselves as major species to balance the equations, as we deem this to be a good means to preserve the chemical features between fullerenes of similar sizes. In this way, it is reasonable to expect a good cancellation of error for the fullerene species in the equations of the isodesmic-type reactions. Furthermore, such an approach would also minimize the total number of species involved, and therefore reduce the error associated with the accompanying species. The remaining consideration is the uncertainty in the smaller fullerenes involved in the reactions. Building on foundation of C_{60}, for which we have estimated an uncertainty of 20.7 kJ mol^{-1}, we expect the Δ_fH values for the higher fullerenes would then have uncertainties of similar magnitudes. The reactions that we employed are

$$C_{70} + 5\ \textit{trans}\text{-butadiene} \rightarrow C_{60} + 5\ \text{benzene} \quad (9)$$

$$'' + 5\ \text{styrene} \rightarrow C_{60} + 5\ \text{naphthalene} \quad (10)$$

$$C_{76} + \text{phenanthrene} \rightarrow C_{70} + \text{corannulene} \quad (11)$$

$$C_{78} + \textit{trans}\text{-butadiene} \rightarrow C_{76} + \text{benzene} \quad (12)$$

$$'' + \text{styrene} \rightarrow C_{76} + \text{naphthalene} \quad (13)$$

$$C_{84} + \text{phenanthrene} \rightarrow C_{78} + \text{corannulene} \quad (14)$$

$$C_{90} + \text{phenanthrene} \rightarrow C_{84} + \text{corannulene} \quad (15)$$

$$C_{96} + \text{phenanthrene} \rightarrow C_{90} + \text{corannulene} \quad (16)$$

The choice of these reactions is based on our examination of a larger set of reactions (see Supporting Information). We note that many of these fullerenes differ in size by six carbon units ($C_{70} \rightarrow C_{76}$ and $C_{78} \rightarrow C_{84} \rightarrow C_{90} \rightarrow C_{96}$). To this end, phenanthrene ($C_{14}H_{10}$) and corannulene ($C_{20}H_{10}$) appear to be a good combination for balancing six carbon atoms due to their modest uncertainty of 2.3 and 4.4 kJ mol^{-1}, respectively. It is noteworthy that they are applied in reaction 7 for the evaluation of the Δ_fH of C_{60}. We can see from Table 3 that the use of ten phenanthrene/corannulene pairs in reaction 7 has led to a standard deviation of 13.3 kJ mol^{-1} in the reaction energies obtained with five DFT and DH-DFT procedures. Thus, it can be expected that, when only one pair is used in an isodesmic-type reaction, the corresponding SD value should be reasonably small. As we shall see, our results for these larger systems indeed indicate a good cancelation of error in the calculated reaction energies when this combination is used with the higher fullerenes.

For fullerenes that differ in size by a number of carbon units that is larger ($C_{60} \rightarrow C_{70}$) or smaller ($C_{76} \rightarrow C_{78}$) than six, we balance the equations using two combinations, namely *trans*-butadiene/benzene and styrene/naphthalene. Each of these pairs serves as a means for balancing a two-carbon unit. We note that there are multiple Δ_fH values reported for styrene from the NIST database. We have thus carried out high-level G4(MP2)-6X,[52] W1X-1[53] and W2X[54] calculations in order to clarify this discrepancy. Our calculated Δ_fH values are in best agreement with the particular reported value of 146.9 ± 1.0 kJ mol^{-1},[55] and we have adopted this experimental value in the present study. Our results (Supporting Information) show that, in all of the cases for which the Δ_fH values can be obtained with reactions using the phenanthrene/corannulene pair, the average of the heats of formation obtained with the *trans*-butadiene/benzene and styrene/naphthalene combinations are quite close to the phenanthrene/corannulene values.

We use the methodologies detailed in the sections above to obtain the Δ_fH values and their associated uncertainties. Thus, the total uncertainties associated with the experimental heats of formation and the theoretical reaction energies are estimated using standard error propagation principles. To estimate the uncertainties associated with our computations, we calculate the reaction energies using B3-PW91-D, BMK-D and DSD-PBE-PBE, and use the approximate correlation in Figure 1 as a rule-of-thumb guide to roughly determine the uncertainties from the standard deviations between the three methods.

We calculate the Δ_fH value of C_{70} as the average of the two values obtained with reactions 9 (butadiene/benzene) and 10 (styrene/naphthalene), and arrive at 2683.4 ± 17.7 kJ mol^{-1} (Table 4). While the heat of formation for C_{78} (2878.8 ± 13.3) is obtained, in a similar manner, as the average of reactions 12 and 13, those for C_{76} (2862.0 ± 18.5), C_{84} (2946.4 ± 14.5), C_{90} (3067.3 ± 15.4) and C_{96} (3156.6 ± 16.2) are calculated with reactions 11, 14, 15 and 16 that employ the combination of phenanthrene and corannulene. We note that the C_{90} fullerene is of particular interest in our scheme as it can potentially serve as a convenient component in isodesmic-type reactions for even larger fullerenes.

DOI: 10.1021/jacs.5b12518
J. Am. Chem. Soc. 2016, 138, 1420−1429

Table 4. Calculated Heats of Formation Values (kJ mol^{-1}) for C_{70}, C_{76}, C_{78}, C_{84}, C_{90} and C_{96} from Reactions 9−16 Obtained with Selected DFT and DH-DFT Procedures in Conjunction with the cc-pVQZ Basis Set

		B3-PW91-D	BMK-D	DSD-PBE-PBE	final proposed value
9	C_{70}	2726.6	2746.2	2697.1 ± 25.3	2683.4 ± 17.7
10	″	2694.7	2701.2	2669.8 ± 24.9	
11	C_{76}	2859.2	2854.7	2862.0 ± 18.5	2862.0 ± 18.5
12	C_{78}	2889.6	2893.8	2881.5 ± 18.8	2878.8 ± 13.3
13	″	2883.2	2884.8	2876.1 ± 18.8	
14	C_{84}	2941.7	2934.2	2946.4 ± 14.5	2946.4 ± 14.5
15	C_{90}	3065.7	3067.4	3067.3 ± 15.4	3067.3 ± 15.4
16	C_{96}	3154.0	3157.3	3156.6 ± 16.2	3156.6 ± 16.2

It is noteworthy that for the three types of reactions employed, i.e., with the *trans*-butadiene/benzene (reactions 9 and 12), styrene/naphthalene (10 and 13) and phenanthrene/coranulene (11, 14−16) pairs, the ranges spanned by the Δ_fH values obtained with three theoretical procedures are not excessively large in many cases. We deem this to be an indication of a reasonable cancellation of error. This may enable computations with decent accuracy using more economical methods, such as hybrid DFT (and perhaps even nonhybrid DFT) procedures, for larger systems that may be taxing even for some of the most advanced computational hardware and software resources.

Large Fullerenes and the Extrapolation to the Graphene Limit. In this section, we calculate the heats of formation for even larger fullerenes (C_{180}, C_{240} and C_{320}), and use these values to examine, on a per-carbon basis, the conceivable convergence behavior of the Δ_fH values. For these systems, the use of a large number of small accompanying species in the isodesmic-type reactions would lead to very significant uncertainties. For example, the equation C_{180} + 14 phenanthrene → C_{96} + 14 corannulene would formally have an uncertainty of 69.5 kJ mol^{-1} associated with the 14 phenanthrene/corannulene pairs. Thus, we employ exclusively the fullerenes themselves for the isodesmic-type reactions. For each of these large fullerenes, we use two reactions to bracket the Δ_fH value.

$$C_{180} \rightarrow 2C_{90} \quad (17)$$

$$'' \rightarrow 3C_{60} \quad (18)$$

$$C_{240} \rightarrow C_{180} + C_{60} \quad (19)$$

$$'' + 1/2C_{60} \rightarrow C_{180} + C_{90} \quad (20)$$

$$C_{320} \rightarrow 4/3C_{240} \quad (21)$$

$$'' + 2/3C_{60} \rightarrow 2C_{180} \quad (22)$$

As we shall see with C_{180} for which DSD-PBE-PBE reaction energies were used in the evaluation of its Δ_fH, although the use of only fullerenes significantly lowers the number of species involved, the relatively large uncertainties of the fullerenes themselves leads to an uncertainty value that is notably larger than the medium-sized fullerenes. We note that the calculations of C_{240} and C_{320} with DH-DFT may be desirable both from the chemical perspective and in terms of pushing the boundary of computational chemistry. However, these large-scale computations are not necessary within the scope of the present study, given that the major use of their Δ_fH values is on a per-atom basis. Thus, for these two largest systems, we employ only the two chosen DFT procedures, namely B3-PW91-D and BMK-D, in the calculations of their Δ_fH. Thus, the average of the four reaction energies (two DFT methods × two isodesmic-type reactions) were used in the calculation of the heats of formation. For these quantities that may be associated with large deviations, for which the values of the uncertainties themselves are perhaps in doubt, we do not attempt to provide an estimation of the associated error bars.

The heats of formation calculated in this manner are 3967.7 ± 33.4 (C_{180}), 4364 (C_{240}) and 5415 (C_{320}) kJ mol^{-1}, respectively (Table 5). Although the uncertainty for C_{180} is large and it is likely that those for C_{240} and C_{320} could be even larger, on a per-carbon basis, these would reduced to just a fraction of a kJ mol^{-1}. For the purpose of investigating the convergence of large fullerenes, we deem such uncertainties quite reasonable. The per-carbon Δ_fH values for all of the fullerenes examined in the present study are shown in Figure 3.

Table 5. Calculated Heats of Formation Values (kJ mol^{-1}) for C_{180}, C_{240} and C_{320} from Reactions 17−22 Obtained with Selected DFT and DH-DFT Procedures[a]

		B3-PW91-D	BMK-D	DSD-PBE-PBE	final proposed value
17	C_{180}	3927.6	3914.0	3968.1 ± 33.8	3967.7 ± 33.4
18	″	3892.2	3911.3	3938.1 ± 63.1	
19	C_{240}	4356	4353		4364
20	″	4379	4366		
21	C_{320}	5350	5429		5415
22	″	5401	5480		

[a]Obtained with the cc-pVQZ basis set for C_{180} and cc-pVTZ for C_{240} and C_{320}.

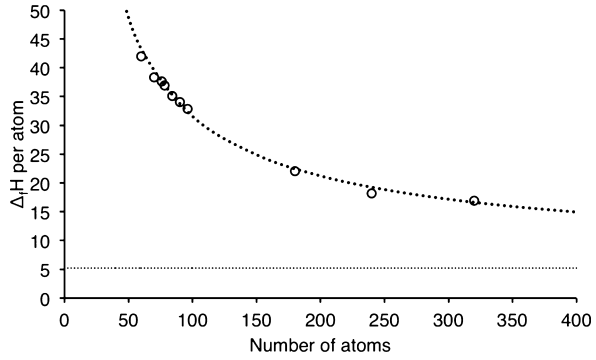

Figure 3. Calculated heats of formation per carbon (kJ mol^{-1}) for C_{60}, C_{70}, C_{76}, C_{78}, C_{84}, C_{90}, C_{96}, C_{180}, C_{240} and C_{320}, showing the slow converging behavior to a limit of 5.2 kJ mol^{-1} with a fit to the equation Δ_fH per carbon = $722n^{-0.72}$ + 5.2 (n = number of carbon atoms).

A formula of the form $E_n = An^{-B} + C$ has previously been employed to estimate the stability of fullerenes (E_n = per-carbon stability energy, n = number of carbon atoms, and A, B and C are adjustable parameters).[3] As we shall see, a formula of this type also seems to fit well to the data in the present study.

What do the per-atom heats of formation and their trend tell us? The reference for the heats of formation is graphite, i.e., multilayered stacking graphene sheets of infinite dimension. Thus, the Δ_fH for an infinitely large single-shelled fullerene consists of two components: (1) the separation of graphite into individual graphene sheets, and (2) the conversion of the sheet

DOI: 10.1021/jacs.5b12518
J. Am. Chem. Soc. 2016, 138, 1420−1429

into a sphere. The energy required for the former process is simply the interlayer binding energy of graphite, with a very recently determined value of 5.2 kJ mol^{-1} per carbon.[56]

We now turn our attention to the second process. One can intuitively deduce that the per-carbon $\Delta_f H$ value of an infinitely large fullerene would approach a "graphene limit",[3] as structural distortions at most of the carbon atoms should progressively become smaller. Indeed, based on bending effects within continuum mechanics treatments, it has been suggested that large fullerenes, regardless of the size, would have a $\Delta_f H$ that differs from the corresponding graphene value by a constant, leading to a zero per-atom difference at the limit.[57] This would suggest a per-carbon heat of formation equaling to the interlayer binding energy of 5.2 kJ mol^{-1}.

As a result, we set the limit of our inverse-power equation to 5.2 kJ mol^{-1}, and fitted the prefactor and the power to the calculated $\Delta_f H$ values per atom. We follow our previous practice[58−60] and minimize the average of the MAD from our data and the SD of these deviations. This yields the formula $\Delta_f H$ per carbon = $722n^{-0.72}$ + 5.2 (kJ mol^{-1}). It can be seen from Figure 3 that C_{320} still has a per-carbon $\Delta_f H$ that differs substantially from the graphene limit. More recent estimations of fullerene heats of formation, obtained by a local curvature model derived using continuum mechanics, are consistent with the results of the present study, with per-carbon $\Delta_f H$ values that are also quite far from the limit for systems up to C_{720}.[61] To this end, our formula suggests a value of 6.2 kJ mol^{-1} for C_{9680}, which comes within 1 kJ mol^{-1} of the graphene-limit value.

What might be the reason for the fairly slow convergence? Fullerenes have 12 pentagons that are connected with one another by hexagons. We hypothesize that these pentagon "vertices" and connected-hexagon "sticks" are likely to be among the most significant bearers of the strains associated with deformation from planarity (Figure 4). Consider a simple

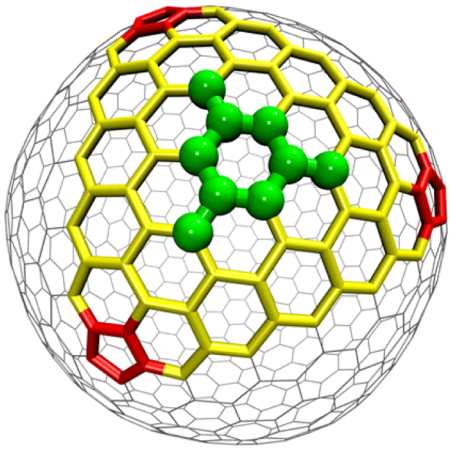

Figure 4. High-strain regions within C_{720} as illustrated by the pentagon "vertices" (red) and the connected-hexagon "sticks" (yellow) that link them. The green ball-and-stick region represents lower-strain areas triangulated by the high-strain ones.

example of fullerenes of type G(0,x) Goldberg polyhedral,[62] there are 12 pentagon vertices linked by 30 connected-hexagon sticks. The two indices in the G(0,x) notation, 0 and x, define the structure of the fullerene, with their sum relating to the length of the connected-hexagon sticks, and 0 signifies that these are "straight" sticks (as opposed to "bended" V-shaped ones). For C_{720} [G(0,6)], there are a total of 540 carbon atoms associated with these high-strain features, and 180 on the lower-strain faces triangulated by the sticks. Thus, the low-strain carbon atoms make up only a quarter of the total.

In general, it can be shown that for a series of large fullerenes of Goldberg polyhedral type G(0,x) with $x \geq 4$, the number of atoms is $20x^2$, the number of high-strain atoms is $60(2x - 3)$, and the number of low-strain atoms is $20(x - 3)^2$. Accordingly, a large increase in the total number of carbon atoms ($20x^2$) is required to bring about a relatively small increase in the proportion of the low-strain structures [$(x - 3)^2/x^2$] within the fullerene. In order for the low-strain regions to cover 95% of the total number of carbon atoms, one must reach x = 119 for C_{283220}! Of course, qualitative schemes for partitioning a structure into low- and high-strain regions may be applicable to other types of nanomaterials, and the distinction between the two types of surfaces may contribute more generally to the unique properties of nanosized substances.

Comparison with Empirical Schemes for Estimating Fullerene $\Delta_f H$. In this second last section, we briefly compare our $\Delta_f H$ values to those obtained by more approximate schemes. Ref 61 provides, through an associated Web site (for which the address is given in its Supporting Information), a list of fullerene heats of formation estimated using its local curvature model. Ref 3 contains the equation E_n = 2206.6 n^{-1} + 36.8 kJ mol^{-1} for the calculation of per-carbon fullerene stabilities (E_n) relative to C_{60}. This equation can be used in conjunction with our C_{60} $\Delta_f H$ to estimate values for other fullerenes. Ref 9 demonstrates an approach that involve the use of simple isodesmic-type reactions together with an economical hybrid-DFT procedure, with an empirical supplementary term associated with the number of carbon and hydrogen atoms in the system of interest. We deem the use of a triple-ζ basis set in their approach still somewhat restrictive computationally, and have redetermined the parameters that are suitable for even less costly procedures using our data. Our exploratory investigation suggests that the B3-PW91-D/cc-pVDZ//PDDG method is quite suitable for the specific purpose of computing fullerene $\Delta_f H$ values.

A summary of our best estimate for the fullerene heats of formation is given in Table 6, together with the deviations from these values for the various more approximate approaches. Of the three methodologies, the local curvature model[61] is

Table 6. Fullerene (C_n) Heats of Formation Values (kJ mol^{-1}) Obtained in the Present Study and Deviations from Them for Those Estimated with Several Approximate Approaches[a]

n	present study	local curvature model[61]	relative stability equation[3]	DFT plus empirical correction[9]
60	2520.0 ± 20.7	−122.4	0.0	8.9
70	2683.4 ± 17.7	−127.9	−111.2	5.6
76	2862.0 ± 18.5	−264.6	−258.4	1.8
78	2878.8 ± 13.3	−306.8	−264.8	7.1
84	2946.4 ± 14.5	−253.9	−301.1	0.3
90	3067.3 ± 15.4	−210.7	−390.6	−1.0
96	3156.6 ± 16.2	−181.4	−448.7	−5.3
180	3967.7 ± 33.4	−20.0	−821.1	−5.9
240	4364	62.2	−903.8	−25.6
320	5415	402.0	−1537.5	23.0

[a]See text for details.

DOI: 10.1021/jacs.5b12518
J. Am. Chem. Soc. 2016, 138, 1420−1429

essentially nonempirical. It takes into account the isomeric form of the fullerene structures, and it is straightforward to apply. The equation of ref 3 has essentially the same form as the one shown in Figure 3, and it is evident from the figure that a simple reparametrization could lead to fairly good agreement with our benchmark data. However, the formula depends only on the number of carbon atoms, and is indifferent to the isomeric structures. The approach of combining DFT, isodesmic-type reactions, and empirical corrections in ref 9 has the potential to provide $\Delta_f H$ estimations that are quite accurate for a wide range of fullerenes. It is, however, the computationally most demanding method to apply.

It is noteworthy that, while there are quantitative discrepancies between the various methods, they all converge to a certain graphene limit. The three approximate methods clearly have their own advantages and shortcomings; we believe further investigations could lead to new approximate schemes that are both accurate and trivially applied. We hope that the relatively more accurate data provided in the present study could in due course contribute to such a development.

Computational Considerations. A large-scale massively parallel resolution-of-identity (RI) MP2 computational study has been carried out previously on the K computer using NTChem.[63] The largest computation in that study involves the RI-MP2/cc-pVTZ calculation of a nanographene dimer ($C_{150}H_{30}$)$_2$. It is associated with 9840 basis functions, 930 occupied and 8910 virtual molecular orbitals, and 26100 auxiliary functions for the RI approximation. That computation was carried out on 71288 cores with a total wall time of 65 min.

In comparison, the DSD-PBE-PBE/cc-pVQZ calculation on C_{180} carried out in the present study involves 9900 basis functions, 540 occupied and 9329 virtual molecular orbitals, and 23760 auxiliary basis functions. Thus, these two computations are comparable in size, with the present study involving one of the largest DH-DFT calculations ever conducted to date. Like the previous RI-MP2 calculation, the C_{180} computation was performed in a massively parallel manner, using 24576 cores in this case with an associated wall time of 228 min. It is noteworthy that, with the efficient RI-MP2 algorithm, the bottleneck for such a large computation is in fact associated with the SCF component (140 min, versus 43 min for the evaluation of RI-MP2 correlation energy).

Since the publication of ref 63, a number of large-scale massively parallel computations on sizable chemical systems using high-level quantum chemistry procedures have been reported, see for example refs 64 and 65 for applications using the MP2-F12 and random-phase-approximation methodologies, respectively. The present study, together with the various previous investigations, illustrates how advances in computer technology enable us to gain a deeper understanding of the fundamentals of large chemical systems using accurate quantum chemistry methodologies that, not very long ago, were not possible.

CONCLUDING REMARKS

In the present study, we have used large-scale computational quantum chemistry calculations, in conjunction with carefully chosen isodesmic-type reactions, to obtain heats of formation that we believe to be among the most accurate theoretical values to date for C_{60}, and the most accurate for some higher fullerenes. They fill in a gap for some of these important species for which experimental $\Delta_f H$ values are not yet available. Our best estimated values are 2520.0 ± 20.7 (C_{60}), 2683.4 ± 17.7 (C_{70}), 2862.0 ± 18.5 (C_{76}), 2878.8 ± 13.3 (C_{78}), 2946.4 ± 14.5 (C_{84}), 3067.3 ± 15.4 (C_{90}), 3156.6 ± 16.2 (C_{96}), 3967.7 ± 33.4 (C_{180}), 4364 (C_{240}) and 5415 (C_{320}) kJ mol^{-1}. These values are calculated mainly using the DSD-PBE-PBE/cc-pVQZ double-hybrid DFT (DH-DFT) procedure, which we find to be the most appropriate method for the purpose of the present study. We also find that the B3-PW91-D3(BJ) and BMK-D3(BJ) functionals perform reasonably well from our assessments. In general, the basis set effect is not excessive between cc-pVTZ and cc-pVQZ for the range of isodesmic-type reactions that we employed.

A finding from our assessment is that, for a set of isodesmic-type reactions for polyaromatic hydrocarbon species, the deviations from high-level benchmark reaction energies seem to correlate fairly well with the spread in the values obtained with a set of relatively accurate DFT and DH-DFT procedures. This provides a convenient mean for the evaluation of isodesmic-type reactions, with small ranges hint at reasonable cancellation of errors by the reaction schemes. In this manner, we find that the isodesmic-type reactions that we employed, which use fullerenes of similar sizes to provide a good balance of the chemistry between the two sides of an equation, as well to minimize the use of accompanying species, are associated with fairly acceptable uncertainties.

The collection of fullerene heats of formation provides a mean to estimate, on a per-carbon basis, the $\Delta_f H$ values for even larger fullerenes by extrapolation to the grapheme limit. Using our best-estimated values, we obtained the formula $\Delta_f H$ per carbon = $722n^{-0.72}$ + 5.2 (kJ mol^{-1}) with n being the number of carbon atoms. The per-carbon heats of formation for fullerenes reach the graphene limit slowly. We rationalize such a convergence behavior by considering the proportion of the "high-strain" regions in simple Goldberg-polyhedra-type fullerenes. By assuming the pentagons and the chains of hexagons that connect them are of higher strain, we reason that it would take fullerenes with over tens (if not hundreds) of thousands of atoms to reasonably approach the limit. This contributes to the distinction between fullerenes and graphene, and further giving these two types of nanomaterials their discrete properties.

ASSOCIATED CONTENT

Supporting Information

The Supporting Information is available free of charge on the ACS Publications website at DOI: 10.1021/jacs.5b12518.

Optimized B3-LYP/6-31G(2df,p) geometries of the fullerenes (as standard XYZ files). (ZIP)

Their zero-point vibrational energies (ZPVE), thermal corrections to enthalpies (ΔH_{298-0}), and electronic energies at selected levels of theory, comparison of ZPVE and ΔH_{298-0} values obtained with different methods, comparison of various quantum chemistry procedures for the estimation of fullerene $\Delta_f H$ using the protocol of ref 9, and heats of formation calculated using various isodesmic-type reactions. (PDF)

AUTHOR INFORMATION

Corresponding Author

*bun.chan@sydney.edu.au

Notes

The authors declare no competing financial interest.

DOI: 10.1021/jacs.5b12518
J. Am. Chem. Soc. 2016, 138, 1420−1429

■ ACKNOWLEDGMENTS

We gratefully acknowledge financial support from Japan Society for the Promotion of Science, Japan (Project 23225001, to K.H.; this project provided a visiting fellowship for B.C.), Ministry of Education, Culture, Sports, Science and Technology, Japan (Grant-in-Aid for Scientific Research on Innovative Areas, Project 15H01006 and Grant-in-Aid for Young Scientists, Project 15K17816, to M.K.), computer time from High Performance Computing Infrastructure, Japan (HPCI General Use of K computer, Junior Researcher Promotion Project HP150186, to M.K.), Research Center for Computational Science, Institute for Molecular Science, Japan (to Y.K.), RIKEN Advanced Center for Computing and Communication, Japan (to B.C.) and National Computational Infrastructure, Australia (to B.C.).

■ REFERENCES

(1) Kroto, H. W.; Heath, J. R.; O'Brien, S. C.; Curl, R. F.; Smalley, R. E. *Nature* **1985**, *318*, 162.
(2) Fowler, P. W.; Manolopoulos, D. E. *An Atlas of Fullerenes*; Dover Publications: Mineola, 2007.
(3) Schwerdtfeger, P.; Wirz, L. N.; Avery, J. *WIREs Comput. Mol. Sci.* **2015**, *5*, 96.
(4) Afeefy, H. Y.; Liebman, J. F.; Stein, S. E. Neutral Thermochemical Data. In *NIST Chemistry WebBook*, NIST Standard Reference Database Number 69; Linstrom, P. J.; Mallard, W. G., Eds.; National Institute of Standards and Technology: Gaithersburg, MD, 2015.
(5) Karton, A.; Chan, B.; Raghavachari, K.; Radom, L. *J. Phys. Chem. A* **2013**, *117*, 1834.
(6) Wan, W.; Karton, A. *Chem. Phys. Lett.* **2016**, *643*, 34.
(7) Wheeler, S. E.; Houk, K. N.; Schleyer, P. v. R.; Allen, W. D. *J. Am. Chem. Soc.* **2009**, *131*, 2547.
(8) Ramabhadran, R. O.; Raghavachari, K. *J. Chem. Theory Comput.* **2011**, *7*, 2094.
(9) Dobek, F. J.; Ranasinghe, D. S.; Throssell, K.; Petersson, G. A. *J. Phys. Chem. A* **2013**, *117*, 4726.
(10) Cioslowski, J.; Rao, N.; Moncrieff, D. *J. Am. Chem. Soc.* **2000**, *122*, 8265.
(11) Wirz, L. N.; Tonner, R.; Hermann, A.; Sure, R.; Schwerdtfeger, P. *J. Comput. Chem.* **2016**, *37*, 10.
(12) Frisch, M. J.; Trucks, G. W.; Schlegel, H. B.; Scuseria, G. E.; Robb, M. A.; Cheeseman, J. R.; Scalmani, G.; Barone, V.; Mennucci, B.; Petersson, G. A.; Nakatsuji, H.; Caricato, M.; Li, X.; Hratchian, H. P.; Izmaylov, A. F.; Bloino, J.; Zheng, G.; Sonnenberg, J. L.; Hada, M.; Ehara, M.; Toyota, K.; Fukuda, R.; Hasegawa, J.; Ishida, M.; Nakajima, T.; Honda, Y.; Kitao, O.; Nakai, H.; Vreven, T.; Montgomery, Jr., J. A.; Peralta, J. E.; Ogliaro, F.; Bearpark, M.; Heyd, J. J.; Brothers, E.; Kudin, K. N.; Staroverov, V. N.; Kobayashi, R.; Normand, J.; Raghavachari, K.; Rendell, A.; Burant, J. C.; Iyengar, S. S.; Tomasi, J.; Cossi, M.; Rega, N.; Millam, N. J.; Klene, M.; Knox, J. E.; Cross, J. B.; Bakken, V.; Adamo, C.; Jaramillo, J.; Gomperts, R.; Stratmann, R. E.; Yazyev, O.; Austin, A. J.; Cammi, R.; Pomelli, C.; Ochterski, J. W.; Martin, R. L.; Morokuma, K.; Zakrzewski, V. G.; Voth, G. A.; Salvador, P.; Dannenberg, J. J.; Dapprich, S.; Daniels, A. D.; Farkas, Ö.; Foresman, J. B.; Ortiz, J. V.; Cioslowski, J.; Fox, D. J. *Gaussian 09*, Revision D.01; Gaussian, Inc.: Wallingford, CT, 2009.
(13) Nakajima, T.; Katouda, M.; Kamiya, M.; Nakatsuka, Y. *Int. J. Quantum Chem.* **2015**, *115*, 349.
(14) Neese, F. *WIREs Comput. Mol. Sci.* **2012**, *2*, 73.
(15) Tománek, D. *Guide Through the Nanocarbon Jungle: Buckyballs, Nanotubes, Graphene, and Beyond*; Morgan & Claypool: San Rafael, 2014.
(16) Bendale, R. D.; Zerner, M. C. *J. Phys. Chem.* **1995**, *99*, 13830.
(17) Margadonna, S.; Brown, C. M.; Dennis, T. J. S.; Lappas, A.; Pattison, P.; Prassides, K.; Shinohara, H. *Chem. Mater.* **1998**, *10*, 1742.
(18) Tamm, N. B.; Troyanov, S. I. *Chem. - Asian J.* **2015**, *10*, 1622.
(19) Yang, S.; Wei, T.; Kemnitz, E.; Troyanov, S. I. *Angew. Chem., Int. Ed.* **2012**, *51*, 8239.
(20) Merrick, J. P.; Moran, D.; Radom, L. *J. Phys. Chem. A* **2007**, *111*, 11683.
(21) Repasky, M. P.; Chandrasekhar, J.; Jorgensen, W. L. *J. Comput. Chem.* **2002**, *23*, 1601.
(22) Kozuch, S.; Martin, J. M. L. *Phys. Chem. Chem. Phys.* **2011**, *13*, 20104.
(23) Grimme, S. *J. Chem. Phys.* **2006**, *124*, 034108.
(24) Karton, A.; Tarnopolsky, A.; Lamère, J. F.; Schatz, G. C.; Martin, J. M. L. *J. Phys. Chem. A* **2008**, *112*, 12868.
(25) Tarnopolsky, A.; Karton, A.; Sertchook, R.; Vuzman, D.; Martin, J. M. L. *J. Phys. Chem. A* **2008**, *112*, 3.
(26) Goerigk, L.; Grimme, S. *J. Chem. Theory Comput.* **2011**, *7*, 291.
(27) Chan, B.; Radom, L. *J. Chem. Theory Comput.* **2011**, *7*, 2852.
(28) Kozuch, S.; Martin, J. M. L. *J. Comput. Chem.* **2013**, *34*, 2327.
(29) Stephens, P. J.; Devlin, F. J.; Chabalowski, C. F.; Frisch, M. J. *J. Phys. Chem.* **1994**, *98*, 11623.
(30) Becke, A. D. *J. Chem. Phys.* **1993**, *98*, 5648.
(31) Yanai, T.; Tew, D. P.; Handy, N. C. *Chem. Phys. Lett.* **2004**, *393*, 51.
(32) Adamo, C.; Barone, V. *J. Chem. Phys.* **1999**, *110*, 6158.
(33) Tao, J. M.; Perdew, J. P.; Staroverov, V. N.; Scuseria, G. E. *Phys. Rev. Lett.* **2003**, *91*, 146401.
(34) Vydrov, O. A.; Scuseria, G. E. *J. Chem. Phys.* **2006**, *125*, 234109.
(35) Schmider, H. L.; Becke, A. D. *J. Chem. Phys.* **1998**, *108*, 9624.
(36) Boese, A. D.; Martin, J. M. L. *J. Chem. Phys.* **2004**, *121*, 3405.
(37) Chai, J.-D.; Head-Gordon, M. *J. Chem. Phys.* **2008**, *128*, 084106.
(38) Zhao, Y.; Truhlar, D. G. *J. Phys. Chem. A* **2005**, *109*, 5656.
(39) Zhao, Y.; Truhlar, D. G. *Theor. Chem. Acc.* **2008**, *120*, 215.
(40) Peverati, R.; Truhlar, D. G. *Phys. Chem. Chem. Phys.* **2012**, *14*, 16187.
(41) Grimme, S.; Ehrlich, S.; Goerigk, L. *J. Comput. Chem.* **2011**, *32*, 1456.
(42) Grimme, S.; Antony, J.; Ehrlich, S.; Krieg, H. *J. Chem. Phys.* **2010**, *132*, 154104.
(43) Grimme, S. *J. Comput. Chem.* **2006**, *27*, 1787.
(44) Martin, J. M. L.; Oliveira, G. *J. Chem. Phys.* **1999**, *111*, 1843.
(45) Martin, J. M. L.; Parthiban, S. W1 and W2 Theory and Their Variants: Thermochemistry in the kJ/mol Accuracy Range. In *Quantum-Mechanical Prediction of Thermochemical Data*; Cioslowski, J., Szarecka, A., Ed.; Kluwer: Dordrecht, 2001; Understanding Chemical Reactivity Series, Vol. *22*, p 31.
(46) Karton, A.; Martin, J. M. L. *J. Chem. Phys.* **2012**, *136*, 124114.
(47) Karton, A.; Daon, S.; Martin, J. M. L. *Chem. Phys. Lett.* **2011**, *510*, 165.
(48) Barnes, E. C.; Petersson, G. A.; Montgomery, J. A., Jr.; Frisch, M. J.; Martin, J. M. L. *J. Chem. Theory Comput.* **2009**, *5*, 2687.
(49) Yang, H.; Mercado, B. Q.; Jin, H.; Wang, Z.; Jiang, A.; Liu, Z.; Beavers, C. M.; Olmstead, M. M.; Balch, A. L. *Chem. Commun.* **2011**, *47*, 2068.
(50) Yang, H.; Jin, H.; Che, Y.; Hong, B.; Liu, Z.; Gharamaleki, J. A.; Olmstead, M. M.; Balch, A. L. *Chem. - Eur. J.* **2012**, *18*, 2792.
(51) Yang, S.; Wei, T.; Kemnitz, E.; Troyanov, S. I. *Chem. - Asian J.* **2014**, *9*, 79.
(52) Chan, B.; Deng, J.; Radom, L. *J. Chem. Theory Comput.* **2011**, *7*, 112.
(53) Chan, B.; Radom, L. *J. Chem. Theory Comput.* **2012**, *8*, 4259.
(54) Chan, B.; Radom, L. *J. Chem. Theory Comput.* **2015**, *11*, 2109.
(55) Prosen, E. J.; Rossini, F. D. *J. Res. NBS* **1945**, *34*, 59.
(56) Wang, W.; Dai, S.; Li, X.; Yang, J.; Srolovitz, D. J.; Zheng, Q. *Nat. Commun.* **2015**, *6*, 7853.
(57) Schmalz, T. G.; Seitz, W. A.; Klein, D. J.; Hite, G. E. *J. Am. Chem. Soc.* **1988**, *110*, 1113.
(58) Chan, B.; Coote, M. L.; Radom, L. *J. Chem. Theory Comput.* **2010**, *6*, 2647.
(59) Chan, B.; Radom, L. *J. Chem. Theory Comput.* **2013**, *9*, 4769.
(60) Chan, B.; Radom, L. *Theor. Chem. Acc.* **2014**, *133*, 1426.

DOI: 10.1021/jacs.5b12518
J. Am. Chem. Soc. 2016, 138, 1420−1429

(61) Guan, J.; Jin, Z.; Zhu, Z.; Chuang, C.; Jin, B.-Y.; Tománek, D. *Phys. Rev. B: Condens. Matter Mater. Phys.* **2014**, *90*, 245403.
(62) Hart, G. Goldberg Polyhedra. In *Shaping Space*, 2nd ed.; Senechal, M., Ed.; Springer: New York, 2012; pp 125−138.
(63) Katouda, M.; Nakajima, T. *J. Chem. Theory Comput.* **2013**, *9*, 5373.
(64) Ohnishi, Y.; Ishimura, K.; Ten-no, S. *Int. J. Quantum Chem.* **2015**, *115*, 333.
(65) Del Ben, M.; Schütt, O.; Wentz, T.; Messmer, P.; Hutter, J.; VandeVondele, J. *Comput. Phys. Commun.* **2015**, *187*, 120.

DOI: 10.1021/jacs.5b12518
J. Am. Chem. Soc. 2016, 138, 1420−1429